Supporting Information

Outstanding Blue Delayed Fluorescent and Significantly Processing Stable Cuprous Complexes with functional pyridine-pyrazolate diimine ligands

Qing Zhang,[a,b,c] Jun Chen,[c] Xiao-Yuan Wu, [a,b] Xu-Lin Chen, [a,b] Rongmin Yu, [a,b] and Can-Zhong Lu *[,a,b]

[a] Key Laboratory of Design and Assembly of Functional Nanostructures, Fujian Institute of Research on the Structure of Matter, Chinese Academy of Sciences；Fuzhou, Fujian 350002, China. Fax: +86-591-8370-5794. E-mail: czlu@fjirsm.ac.cn.

[b] Fujian Provincial Key Laboratory of Nanomaterials, Fujian Institute of Research on the Structure of Matter, Chinese Academy of Sciences.

[c] Graduate University of Chinese Academy of Sciences, Beijing 100049, China.

Experimental section

General procedures: Reagents and solvents were purchased from commercial sources and used without further purification. All reactions were performed under N_2 atmosphere using standard Schlenk techniques unless specified. The complex $[Cu(CH_3CN)_4]BF_4$[1] was prepared according to literature procedures. ^1H NMR and ^{31}P NMR spectra were recorded on a Bruker Avance III 400 MHz NMR spectrometer. Elemental analyses (C, H, N) were carried out with an Elementar Vario EL III elemental analyzer.

Synthesis

2-methyl-6-(1H-pyrazol-3-yl)pyridine (A) According to literature[2] (Fig. S1), a mixture of 2-acetylpyridine (10 g) and dimethylformamide dimethyl acetal (25 mL) was refluxed for 16 h into a dark brown solution. After the removal of excess solvent under vacuum, the crude brown oil was recrystallized from $CHCl_3$/petroleum ether to give 3-dimethylamino-1-(pyridine-2-yl)prop-2-en-1-one (**B**) as yellow crystalline solid (12 g). Then, **B** was added to a solution of hydrazine monohydrate (15 mL) in ethanol. The mixture was refluxed for 30 min. The solvent was removed under vacuum to get white solid, which further purified through crystallization in $CHCl_3$/petroleum ether to give colourless crystal.

2-methyl-6-(1-R-phenyl-1H-pyrazol-3-yl)pyridine. This preparation process is in accordance with a revised method[3]. A (0.3 g, 2.07 mmol), 1, 10-phenanthroline (0.149 g, 0.827 mmol), copper(I) iodide (0.079 g, 0.413 mmol), caesium carbonate (1.35 g, 4.13 mmol), 2.07mmol iodobenzene for **L1**, 2-methyl iodobenzene for **L2**, 4-methyl iodobenzene for **L3**, 2-trifluoromethyl iodobenzene for **L4** and 4-trifluoromethyl iodobenzene for **L5** were dissolved in dry DMF (10 mL). The mixture was stirred vigorously for 1 h at room temperature and then heated to 100 ºC under nitrogen for another 36 h. At room temperature, the residue was filtrated. The liquid phase was extracted with CH_2Cl_2 (3 × 30 mL) and washed with water, subsequently dried with anhydrous sodium sulphate. After the removal of solvent under vacuum, the crude product was purified by column chromatography on silica gel with ethyl acetate/petroleum ether.

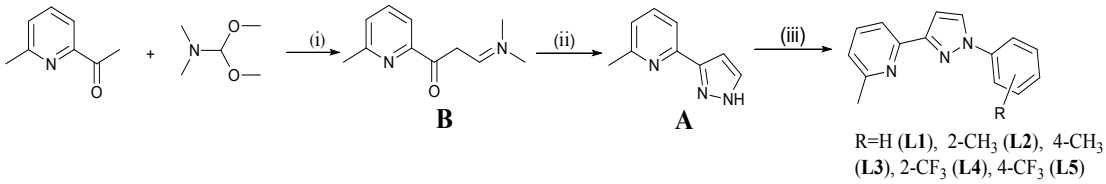

Fig. S1. Synthesis of diamine ligands. (i) Reflux, 16 h. (ii) 2 eq of hydrazine hydrate in ethanol, reflux for 2 h. (iii) 0.2 eq of cuprous iodine, 0.4 eq of 1,10-phenanthroline, 1 eq of benzene halide and 2 eq of cesium carbonate, under nitrogen, at 100 ºC, 24 h.

Cuprous complexes. The five cuprous complexes were prepared according to the following procedures: A mixture of $[Cu(CH_3CN)_4]BF_4$ (1 mmol) and phosphine ligand

(POP, 1 mmol) in CH_2Cl_2 (10 mL) was stirred at room temperature for 0.5 h. Then, corresponding diimine ligands were added. The solvent was evaporated after the reaction mixture was stirred for another 1 h. Then, single crystal of **1** for X-ray diffraction was obtained through slowly volatilization of saturated ethanol solutions, and the others were obtained through the diffusion of diethyl ether into CH_2Cl_2 solutions of the products.

Cu(L1)(POP)BF_4 (1). ^{1}H NMR (400 MHz, $CDCl_3$): δ 8.00 (s, 1H), 7.95 (d, 2H), 7.38 (t, 4H), 7.25 – 7.19 (m, 7H), 7.16 (t, 2H), 7.11 – 7.03 (m, 8H), 6.95-6.91 (m, 6H), 6.87-6.79 (m, 6H), 6.61-6.60 (m, 2H), 1.78 (s, 3H). ^{31}P NMR: -14.09 (s). Anal. Calcd for $C_{51}H_{41}BCuF_4N_3OP_2$: C, 66.28; H, 4.47; N, 4.55. Found: C, 66.15; H, 4.30; N, 4.46.

Cu(L2)(POP)BF_4 (2). ^{1}H NMR (400 MHz, $CDCl_3$): δ 8.03–7.96 (m, 2H), 7.71 (d, 1H), 7.43–7.30 (m, 6H), 7.23–7.17 (m, 7H), 7.12–7.08 (m, 5H), 6.93 (t, 3H), 6.88–6.80 (m, 9H), 6.72 (d, 1H), 6.59-6.55 (m, 2H), 1.73 (s, 3H), 1.58 (s, 3H). ^{31}P NMR: -14.58 (s). Anal. Calcd for $C_{52}H_{43}BCuF_4N_3OP_2$: C, 66.57; H, 4.62; N, 4.48. Found: C, 66.22; H, 4.41; N, 4.44.

Cu(L3)(POP)BF_4 (3). H NMR (400 MHz, $CDCl_3$): δ 7.98–7.93 (m, 3H), 7.38 (t, 2H), 7.31 (s, 1H), 7.27–7.20 (m, 6H), 7.18–7.16 (m, 2H), 7.15–7.04 (m, 5H), 6.95–6.90 (m, 8H), 6.87–6.83 (m, 6H), 6.79 (d, 2H), 6.62-6.58 (m, 2H), 2.20 (s, 3H), 1.77 (s, 3H). ^{31}P NMR: -14.00 (s). Anal. Calcd for $C_{52}H_{43}BCuF_4N_3OP_2$: C, 66.57; H, 4.62; N, 4.48. Found: C, 66.12; H, 4.31; N, 4.43.

Cu(L4)(POP)BF_4 (4). H NMR (400 MHz, $CDCl_3$): δ 8.0 (d, 1H), 7.75–7.71 (t, 2H), 7.53 (t, 2H), 7.38–7.31 (m, 6H), 7.25–7.19 (m, 7H), 7.15–7.10 (m, 4H), 7.01 – 6.95 (m, 3H), 6.93–6.86 (m, 8H), 6.81 (d, 2H), 6.70–6.66 (m, 2H), 1.84 (s, 3H), 3.50 (dd, 1H), 1.3 (t, 1.5H). ^{31}P NMR: -14.72 (s). Anal. Calcd for $C_{52}H_{40}BCuF_7N_3OP_2$: C, 62.95; H, 4.06; N, 4.24. Found: C, 62.54; H, 4.10; N, 4.13.

Cu(L5)(POP)BF_4 (5). H NMR (400 MHz, $CDCl_3$): δ 8.27 (d, 1H), 7.97 (d, 2H), 7.41–7.35 (m, 6H), 7.26–7.23 (m, 4H), 7.19 – 7.13 (m, 4H), 7.06 (t, 4H), 6.99–6.95 (m, 7H), 6.86–6.79 (m, 7H), 6.70-6.68 (m, 2H), 1.85 (s, 3H). ^{31}P NMR: -13.99 (s). Anal. Calcd for $C_{52}H_{40}BCuF_7N_3OP_2$: C, 62.95; H, 4.06; N, 4.24. Found: C, 62.66; H, 3.97; N, 4.27.

X-ray Crystallographic Analysis: Diffraction data of complexes **1, 4** and **5** were collected on a SuperNova, Dual, Cu at zero, Atlas diffractometer equipped with graphite-monochromated Cu Kα radiation (λ =1.54184 Å). Diffraction data of complexes **2** and **3** were collected on a Saturn724 CCD Rigaku Mercury and a diffractometer equipped with graphite-monochromated Mo Kα radiation (λ = 0.71073 Å), respectively. Structures were solved by direct methods and refined by full-matrix least-squares methods with SHELXL-97 program package. Hydrogen atoms were added in idealized positions. All nonhydrogen atoms were refined anisotropically. Details of crystal and structure refinement are listed in Table S1, selected bond length and angles are displayed in Table S2 and the OPRET diagrams of these complexes are shown in Fig. S2. CCDC 1047202–1047206 contain the supplementary crystallographic data for complexes **1**–**4** respectively.

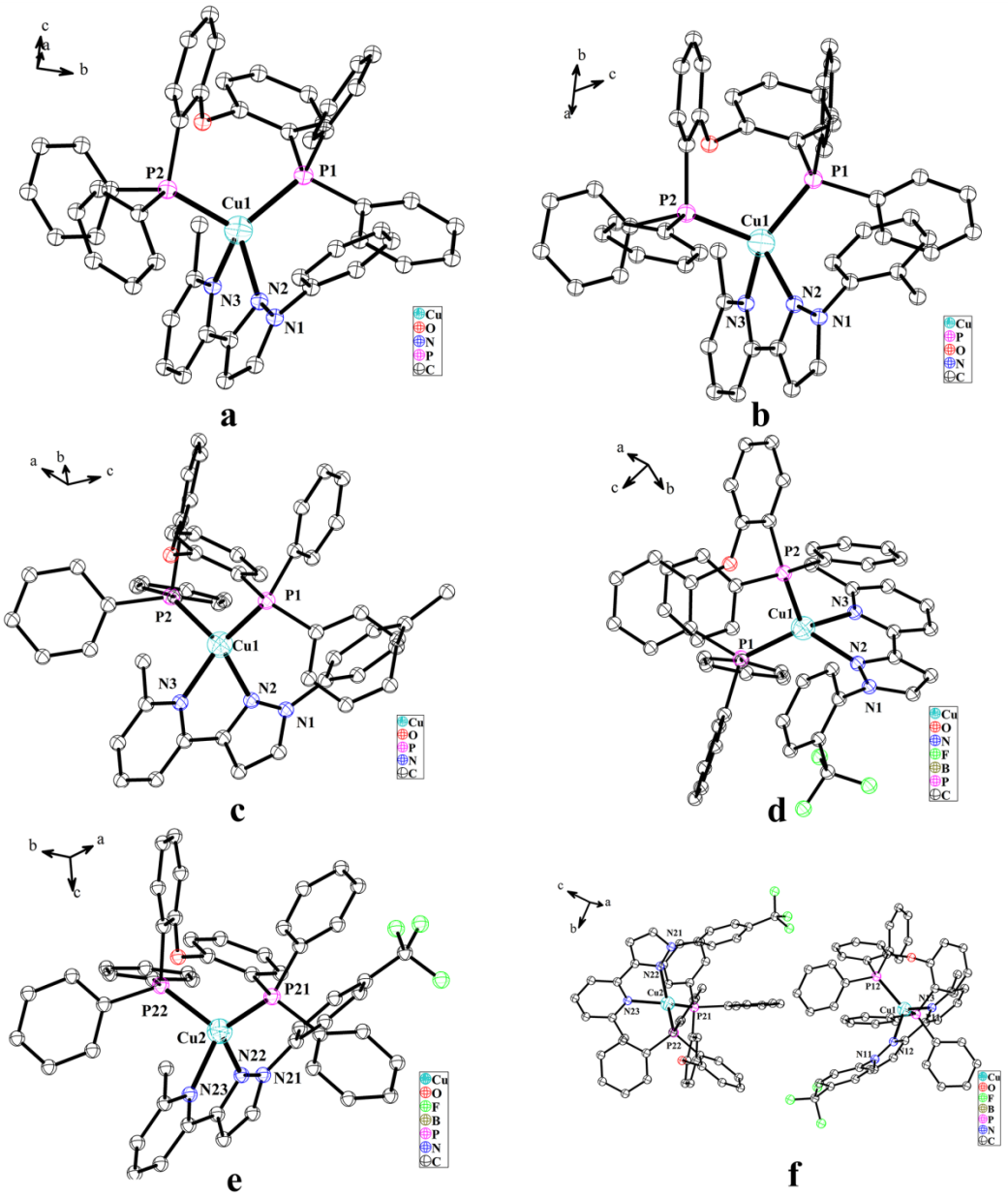

Fig. S2. ORTEP diagrams of **1** (**a**), **2** (**b**), **3** (**c**), **4** (**d**) and **5** (**e, f**) with thermal ellipsoids at a 30% probability level. Solvent molecules, the anion, and H atoms are omitted for clarity.

Table S1. Crystallographic data and structural refinements for **1–5.**

	1	**2**	**3**	**4**	**5**
Formula	$C_{51}H_{41}BCuF_4N_3OP_2$	$C_{52}H_{43}BCuF_4N_3OP_2$	$C_{52}H_{43}BCuF_4N_3OP_2$	$C_{54}H_{45}BCuF_7N_3O_2P_2$	$C_{52}H_{40}BCuF_7N_3OP_2$
***M*$_r$ (g mol^{-1})**	924.16	938.18	938.18	1037.22	1984.32
Space group	$P2_1$	Cc	Cc	$Pccn$	$Pca2_1$
***a*/Å**	10.1555(2)	24.905(5)	24.814(9)	22.9494(3)	20.7888(3)
***b*/Å**	14.5701(3)	15.045(3)	15.188(5)	19.5135(2)	13.5681(2)
***c*/Å**	14.7592(3)	15.151(3)	15.388(6)	21.4611(2)	32.2236(4)

α/°	90	90	90	90	90
β/°	92.645(2)	127.405(3)	128.114(6)	90	90
γ/°	90	90	90	90	90
V/Å^3	2181.54(8)	4509.6(15)	4563(3)	9610.78(18)	9089.1(2)
Z	2	4	4	8	4
D_c/g cm^{-3}	1.407	1.382	1.366	1.434	1.450
μ/mm^{-1}	1.898	0.615	0.607	1.895	1.961
F(000)	952	1936	1936	4256	4064
total reflns	8183	21594	21614	24177	22565
unique reflns	5758	10134	9069	9095	12720
R_{int}	0.0155	0.0241	0.0299	0.0217	0.0213
GOF	1.002	0.949	0.930	0.991	1.004
R_1[a][$I>2\sigma(I)$]	0.0242	0.0379	0.0453	0.0676	0.0387
wR_2[b](all data)	0.0736	0.1061	0.1296	0.2111	0.1172
CCDC	1047202	1047203	1047204	1047205	1047206
[a]$R_1 = \sum(F_o - F_c) / \sum F_o$; [b]$wR_2 = [\sum w(F_o^2 - F_c^2)^2 / \sum w(F_o^2)^2]^{1/2}$.					

Table S2. Selected bond lengths (Å) and angles (º) for **1**–**5.**

1			
Cu(1)-N(3)	2.1024(17)	Cu(1)-P(1)	2.2544(5)
Cu(1)-N(2)	2.1428(16)	Cu(1)-P(2)	2.2982(6)
N(3)-Cu(1)-N(2)	78.30(6)	N(3)-Cu(1)-P(2)	109.00(5)
N(3)-Cu(1)-P(1)	120.22(5)	N(2)-Cu(1)-P(2)	114.03(5)
N(2)-Cu(1)-P(1)	117.03(5)	P(1)-Cu(1)-P(2)	113.66(2)
2			
Cu(1)-N(3)	2.084(2)	Cu(1)-P(1)	2.2636(7)
Cu(1)-N(2)	2.164(2)	Cu(1)-P(2)	2.2842(7)
N(3)-Cu(1)-N(2)	79.23(10)	N(3)-Cu(1)-P(2)	108.20(6)
N(3)-Cu(1)-P(1)	123.02(7)	N(2)-Cu(1)-P(2)	116.03(6)
N(2)-Cu(1)-P(1)	116.02(6)	P(1)-Cu(1)-P(2)	111.14(3)
3			
Cu(1)-N(3)	2.108(3)	Cu(1)-P(1)	2.2565(11)
Cu(1)-N(2)	2.132(3)	Cu(1)-P(2)	2.2912(13)
N(3)-Cu(1)-N(2)	78.69(13)	N(3)-Cu(1)-P(2)	107.66(10)
N(3)-Cu(1)-P(1)	124.49(10)	N(2)-Cu(1)-P(2)	115.32(9)
N(2)-Cu(1)-P(1)	118.14(9)	P(1)-Cu(1)-P(2)	109.64(3)
4			

Cu1-N3	2.153(3)	Cu1-P2	2.2808(10)
Cu1- N2	2.153(3)	Cu1-P1	2.2976(10)
N3-Cu1-N2	78.06(12)	N3-Cu1-P1	117.06(9)
N3-Cu1 -P2	115.34(9)	N2-Cu1-P1	126.03(9)
N2 -Cu1-P2	108.85(9)	P2-Cu1-P1	108.87(4)
5			
Cu(1)-N(13)	2.119(3)	Cu(2)-N(23)	2.107(3)
Cu(1)-N(12)	2.153(2)	Cu(2)-N(22)	2.177(2)
Cu(1)-P(11)	2.2682(7)	Cu(2)-P(21)	2.2573(7)
Cu(1)-P(12)	2.2918(8)	Cu(2)-P(22)	2.2917(8)
N(13)-Cu(1)-N(12)	78.58(9)	N(23)-Cu(2)-N(22)	78.82(10)
N(13)-Cu(1)-P(11)	121.44(7)	N(23)-Cu(2)-P(21)	121.07(7)
N(12)-Cu(1)-P(11)	121.12(7)	N(22)-Cu(2)-P(21)	120.58(7)
N(13)-Cu(1)-P(12)	106.83(7)	N(23)-Cu(2)-P(22)	106.23(7)
N(12)-Cu(1)-P(12)	109.69(7)	N(22)-Cu(2)-P(22)	108.76(7)
P(11)-Cu(1)-P(12)	113.96(3)	P(21)-Cu(2)-P(22)	115.55(3)

Thermogravimetric analysis (TGA) experiments: TGA were done on a NETZSCH STA 449C Jupiter thermogravimetric analyzer in flowing nitrogen with the sample heated in an Al_2O_3 crucible at a heating rate of 10 $Kmin^{-1}$ (Fig. S3). The samples used for experiment have been dried at 90ºC for 30min. The weight loss for complex **4** under 200ºC belongs to the release of diethyl ether. And the thermostability for these five complexes are up to 350ºC.

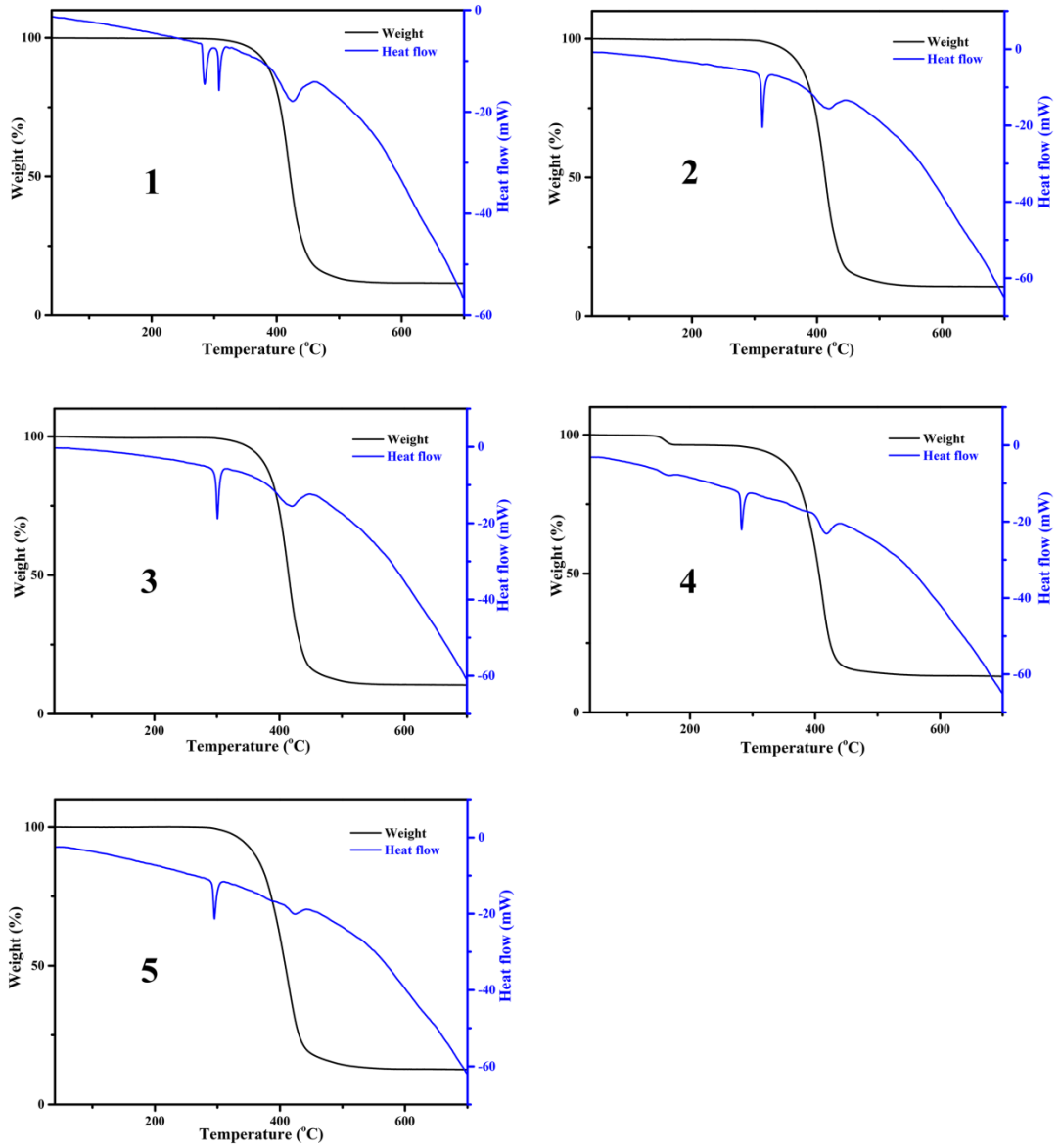

Fig. S3 TGA and heat flow curves for **1**–**5**.

Photophysical Measurements: The solution samples for the photophysical studies were carefully degassed. The film samples were prepared by spin-coating a mixture of the cuprous complex and poly(methyl methacrylate) (PMMA) in distilled CH_2Cl_2 onto a quartz glass slide. All the film samples were dried under vacuum at 50 °C for 2 h before photophysical measurements. The powder samples were obtained by drying the crystals and measured without further treatment. UV−vis absorption spectra were recorded with a Perkin- Elmer Lambda 45 UV/vis spectrophotometer. Photoluminescence spectra at room temperature and 77 K were recorded on a HORIBA Jobin-Yvon FluoroMax-4 spectrometer and an Edinburgh Analytical instrument FLS920, respectively. The lifetimes of solution samples were measured by the time-correlated single-photon counting (TCSPC) upgrade on the FluoroMax-4 spectrometer with a FluoroHub module. The lifetimes of powder samples at different temperatures were performed on an Edinburgh Analytical instrument FLS920 with a Picosecond Laser Diode. The powder and thin film PL quantum yields were defined as the number of photons emitted per photon absorbed by the systems and measured by FluoroMax-4 equipped with an integrating sphere. The

corresponding optical behaviors are shown in Fig. S4–S11 and Table S3.

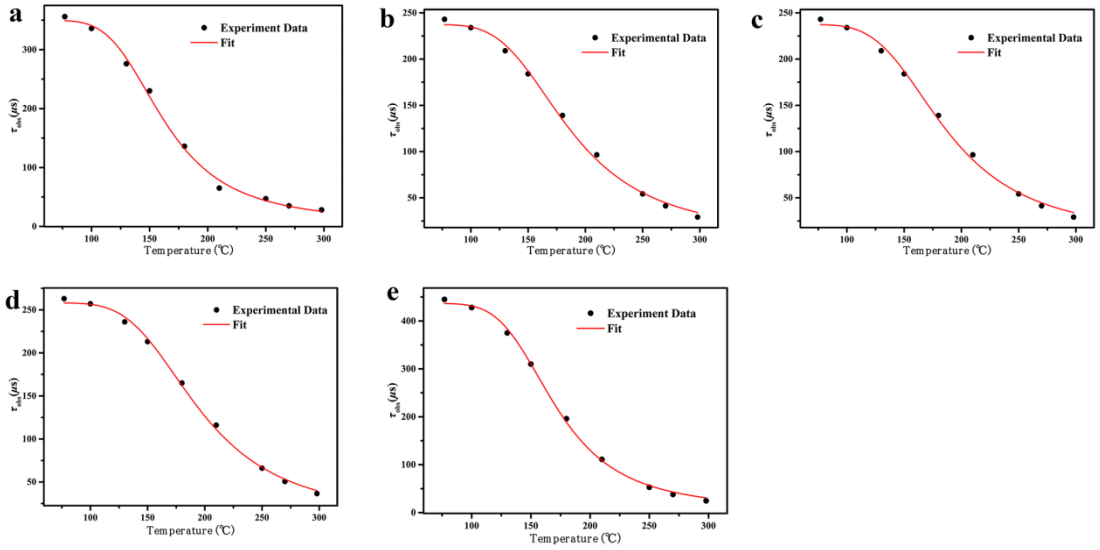

Fig. S4 Life times for **1**–**5** at various temperatures and their fitted curves.

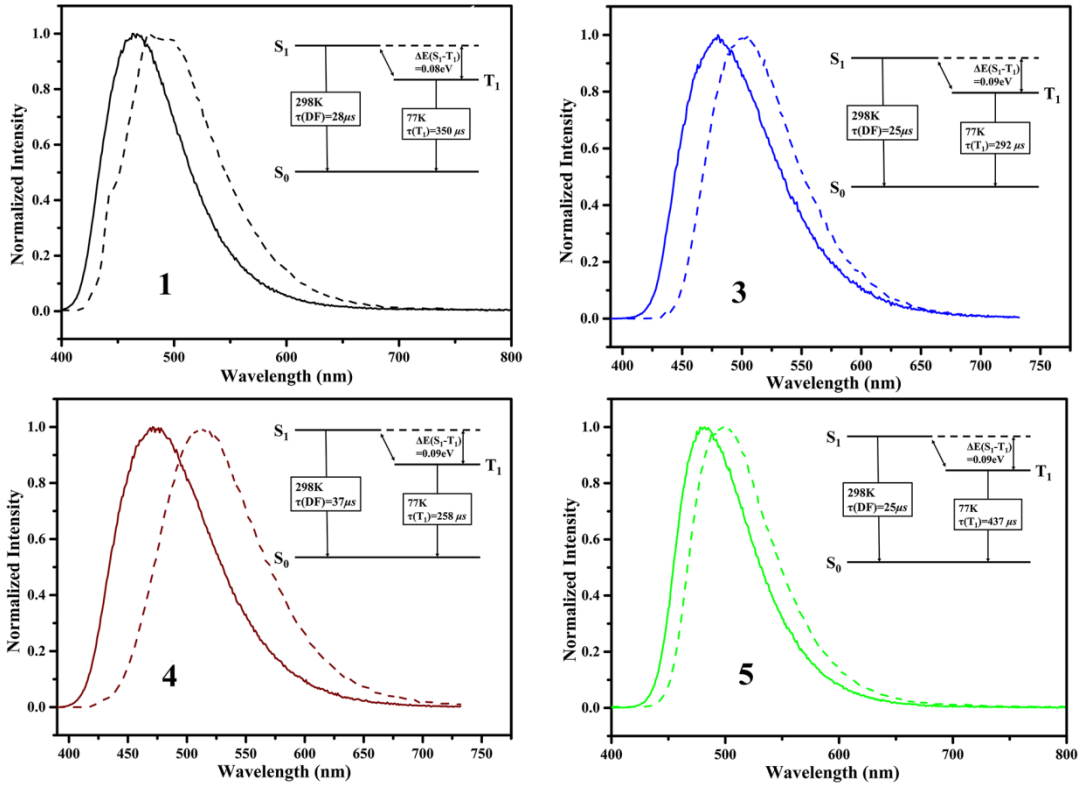

Fig. S5 Emission spectra of **1**, **3**, **4** and **5** in the solid state at 293 K (solid) and 77 K (dashed). The inset displays the energy gap between S_1 and T_1 levels of them.

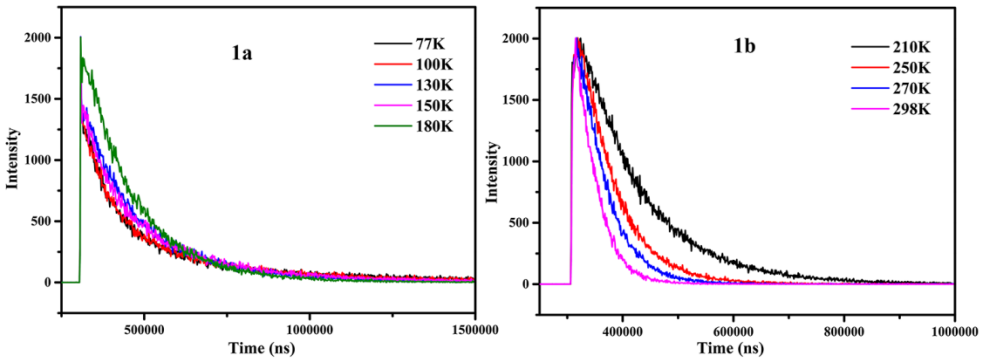
1a
77K
100K
130K
150K
180K
Intensity
Time (ns)
1b
210K
250K
270K
298K
Intensity
Time (ns)

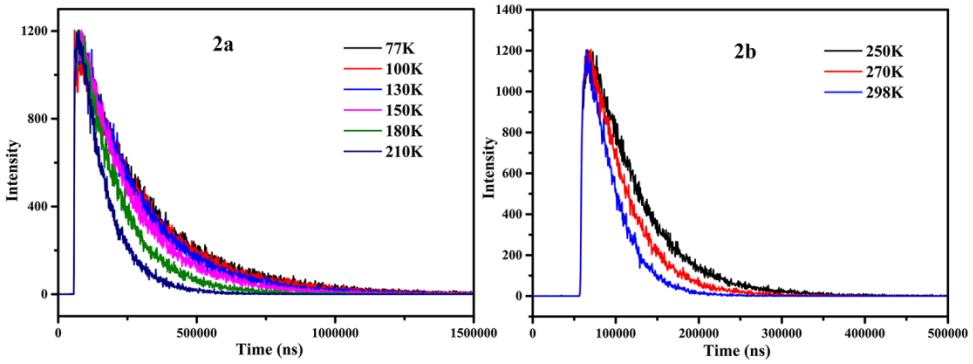
2a
77K
100K
130K
150K
180K
210K
Intensity
Time (ns)
2b
250K
270K
298K
Intensity
Time (ns)

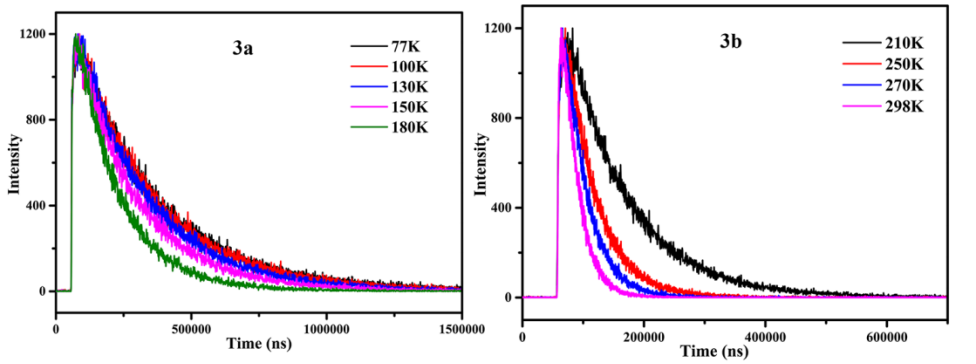
3a
77K
100K
130K
150K
180K
Intensity
Time (ns)
3b
210K
250K
270K
298K
Intensity
Time (ns)

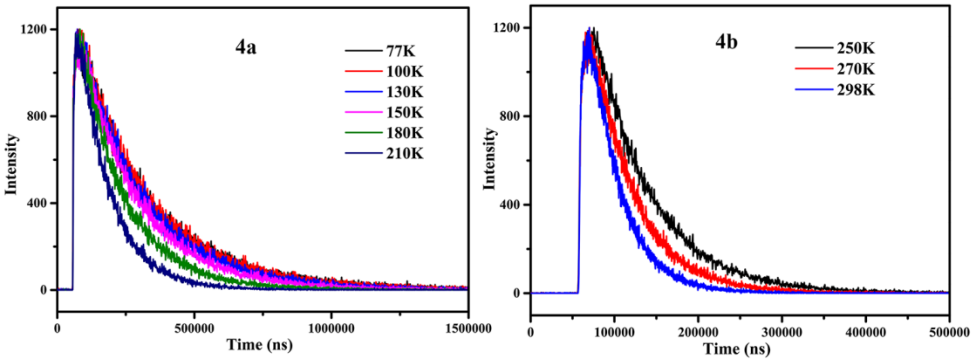
4a
77K
100K
130K
150K
180K
210K
Intensity
Time (ns)
4b
250K
270K
298K
Intensity
Time (ns)

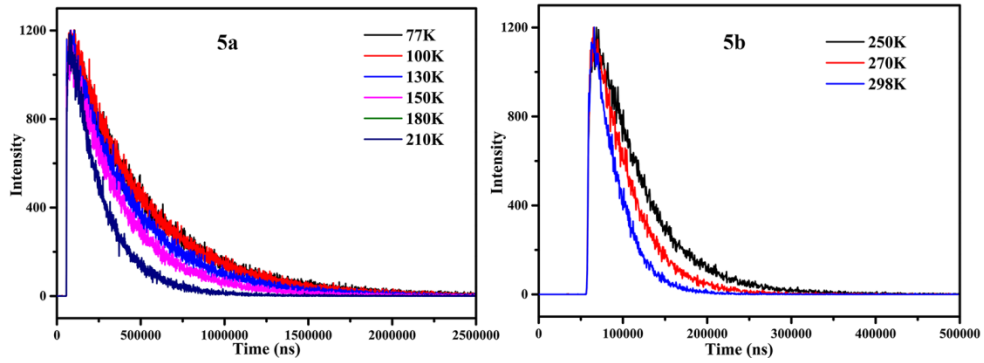
5a
77K
100K
130K
150K
180K
210K
Intensity
Time (ns)
5b
250K
270K
298K
Intensity
Time (ns)

Fig. S6 Decay curves for **1**–**5** in solid state at various temperatures.

Table S3. Life times for **1**–**5** in solid state at various temperatures.

	Life Time (μs)								
	77K	100K	130K	150K	180K	210K	250K	270K	298K
1	356	336	276	230	136	65	47	35	28
2	243	234	209	184	139	97	54	41	29
3	298	289	260	227	161	97	49	36	25
4	263	257	236	213	165	116	66	51	37
5	445	428	375	310	196	111	53	38	25

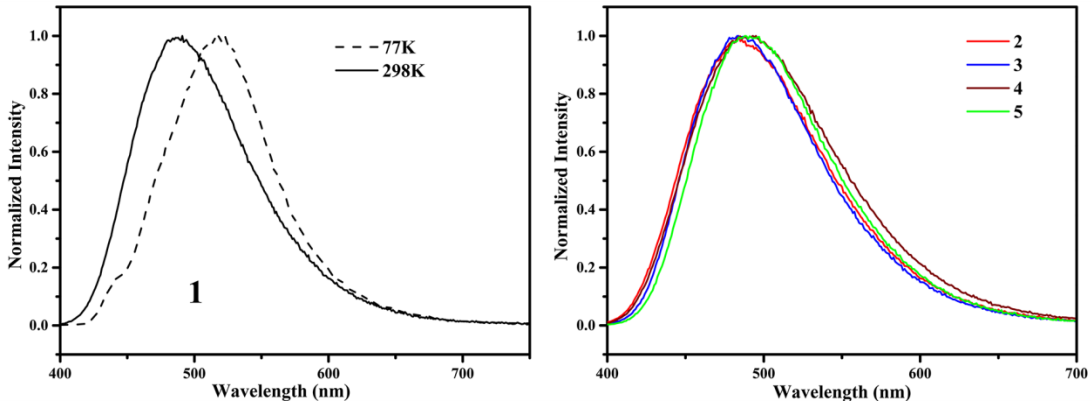

Fig. S7 The emission curves for **1** in thin film at 77K and 298K (Left). The emission curves for **2**–**5** in thin film at 298K (Right).

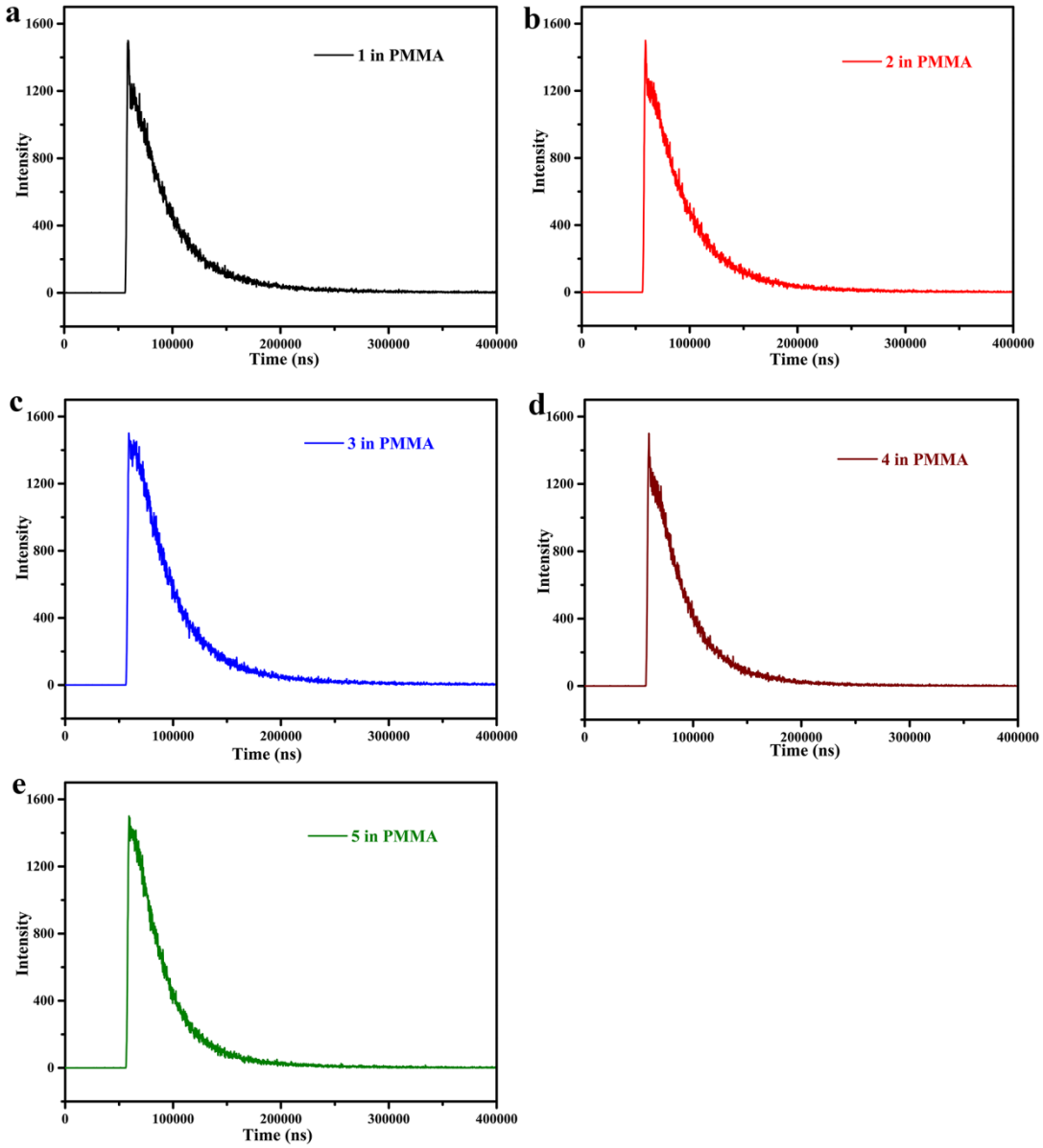

Fig. S8 Decay curves for **1**–**5** in PMMA at 298K.

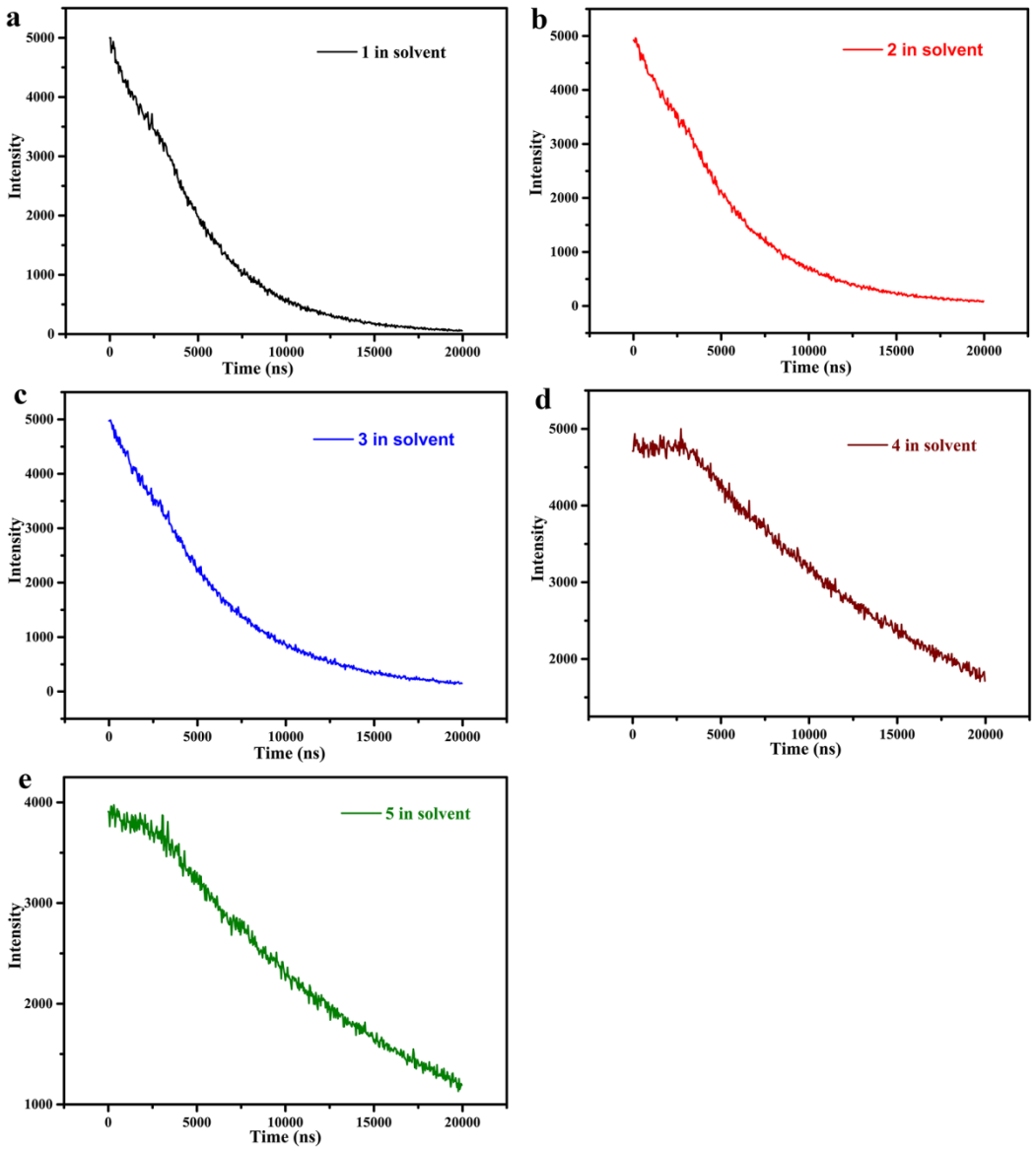

Fig. S9 Decay curves for **1**–**5** in degassed CH_2Cl_2 solution at 298K.

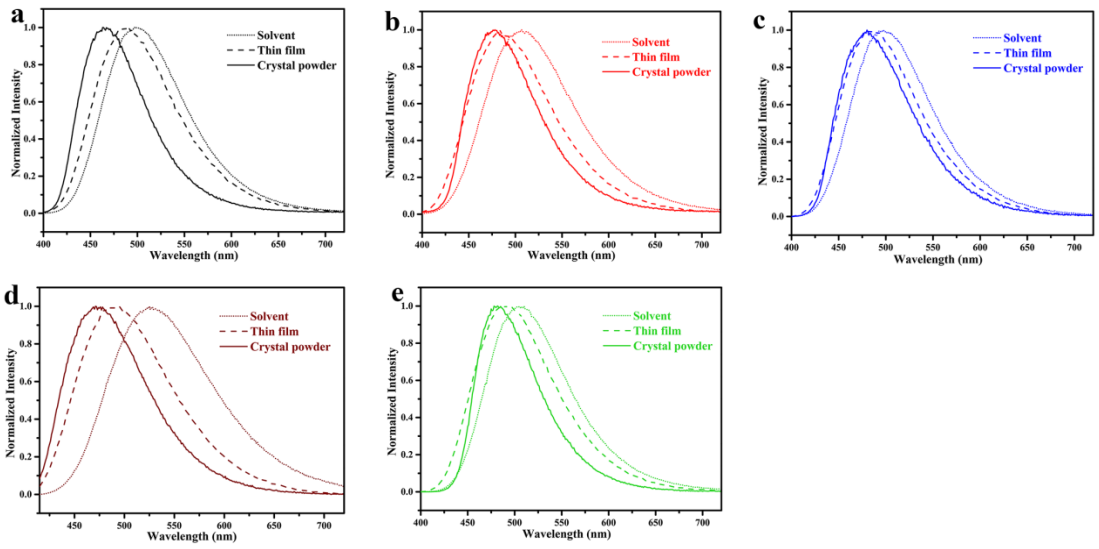

Fig. S10 Emission curves of crystal powder, thin film and solvent for **1** (**a**), **2** (**b**), **3** (**c**), **4** (**d**) and

5 (**e**).

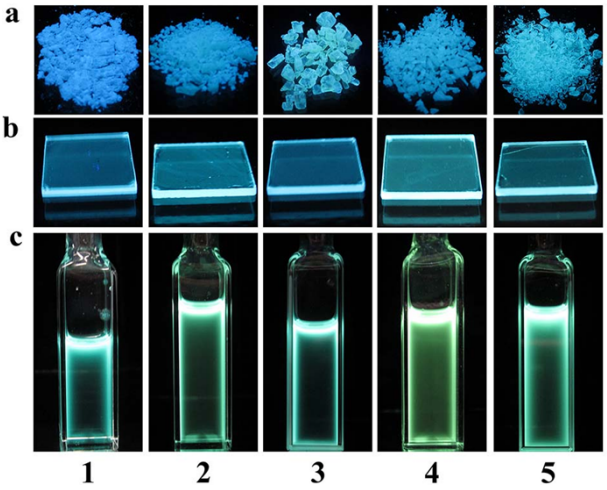

Fig. S11 Photographs of **1**–**5** in various matrix.

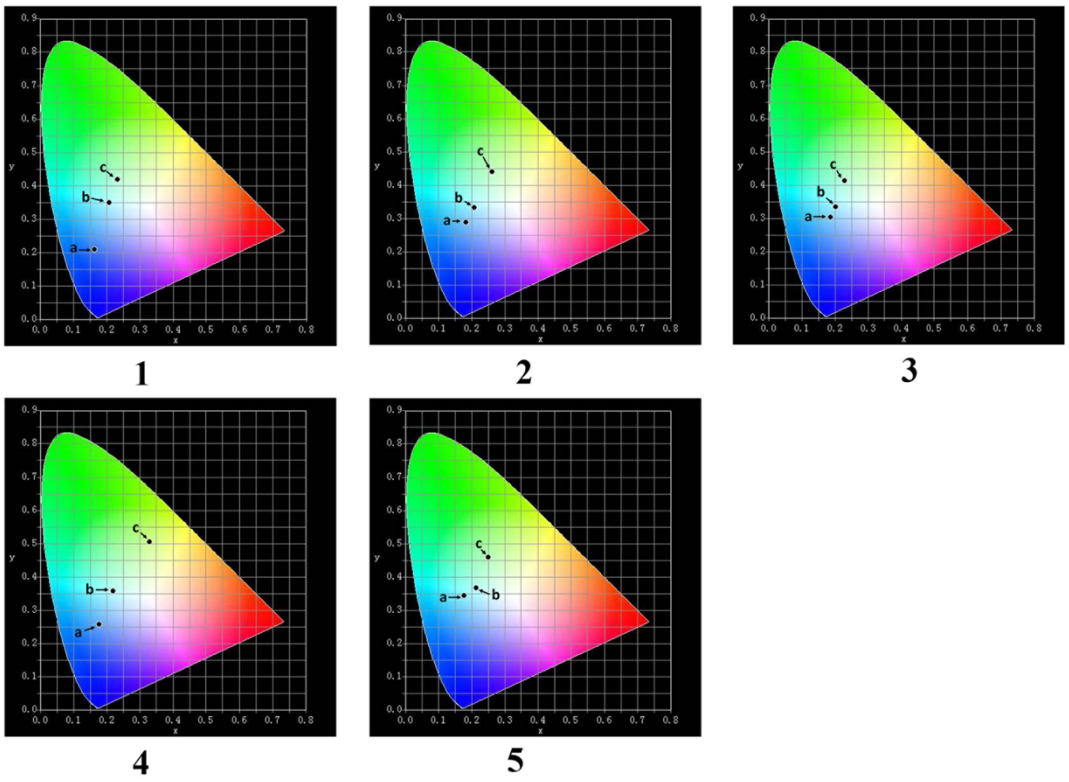

Fig. S12 CIE graphs of **1**–**5. a, b, c** depicts these complexes in crystal state, thin film and solvent, respectively.

Table S4 The CIE coord of **1**–**5** in crystal, thin film and solvent.

	CIE		
	Crystal	Thin film	solvent
1	(0.16, 0.21)	(0.21, 0.35)	(0.23, 0.42)
2	(0.18, 0.29)	(0.21, 0.33)	(0.26, 0.44)
3	(0.17, 0.30)	(0.20, 0.33)	(0.23, 0.41)
4	(0.18, 0.26)	(0.22, 0.36)	(0.33, 0.50)
5	(0.18, 0.34)	(0.21, 0.37)	(0.25, 0.46)

1 G. J. Kubas, *Inorg. Syn.*, 1979, **XIX**, 3.
2 Z. R. Reeves, K. L. V. Mann, J. C. Jeffery, J. A. McCleverty, M. D. Ward, F. Barigelletti and N. Armaroli, *J. Chem. Soc., Dalton Trans.*, 1999, 349.
3 G.-G. Shan, H.-B. Li, D.-X. Zhu, Z.-M. Su and Y. Liao, *J. Mater. Chem.*, 2012, **22**, 12736.